Engineering the quantum point contact response to single-electron charging in a few-electron quantum-dot circuit

L.-X. Zhang and J. P. Leburton[a)]
Beckman Institute for Advanced Science & Technology and Department of Electrical and Computer Engineering, University of Illinois at Urbana-Champaign, Urbana, Illinois 61801

R. Hanson and L. P. Kouwenhoven
Department of NanoScience and ERATO Mesoscopic Correlation Project, Delft University of Technology, P.O. Box 5046, 2600 GA Delft, The Netherlands

(Received 3 May 2004; accepted 15 July 2004)

We show that the design of a quantum point contact adjacent to a quantum dot can be optimized to produce maximum sensitivity to single-electron charging in the quantum dot. Our analysis is based on the self-consistent solution of coupled three-dimensional Kohn-Sham and Poisson equations for the quantum circuit. We predict a detection sensitivity increase by at least 73% over the conventional design. © *2004 American Institute of Physics*. [DOI: 10.1063/1.1790605]

Quantum point contact (QPC) is a constricted one-dimensional (1D) conduction channel formed by properly biasing two closely separated metal gates on top of a two-dimensional electron gas (2DEG) at the interface of a semiconductor heterostructure (e.g., GaAs/AlGaAs). In the low-temperature regime, the QPC conductance is quantized in units of $2e^2/h$, which is the signature of ballistic transport in the mesoscopic constriction.[1,2] Recently, it was shown that a QPC can be placed adjacent to a planar quantum dot (QD) and used as a sensitive detector to read the charge state in the QD.[3] Biasing the QPC gates such that its conductance is $G=e^2/h$ (which is halfway between pinch off and the first conductance plateau $G_0=2e^2/h$) gives a maximum conductance sensitivity to the electrostatic environment. Hence, it is possible to detect sudden changes in the QPC conductance induced by single-electron charging in the QD down to its depletion of electrons.[4,5] Single-quantum measurement achieved in this type of circuit is an important step towards the realization of electronic devices for quantum information processing.[6] Therefore, for systematic measurements of quantum systems, optimum detection sensitivity is desirable.

In this letter, we show that the QPC can be properly designed to enhance the detector sensitivity to the single-electron charging in a QD near it. In doing so, we compute, for four designs of the QPC gate geometry, the detector sensitivity in terms of the relative change of the QPC conductance ($\Delta G/G$) when a single electron is placed in the adjacent QD. The original design of the QPC-QD system is represented in Fig. 1 where two QPC readouts are integrated with a laterally coupled quantum dot (LCQD) structure to form a quantum circuit.[5] Figure 1(a) shows the top view of the metal gates, properly biased such that the LCQD (shown by two circles) are well defined by the *L*, *R*, *T*, and *M* gates. The QPC's are formed via the tips between $L(R)$ and QPC$-L$ (QPC$-R$) gates. The PL and PR gates are plunger gates that are used for fine tuning the potential in the two dots, thereby controlling precisely the charge state down to a single electron in the QD's.[5] In Fig. 1(a), curved arrows show the charging paths, whereas QPC currents are shown by straight arrows. A cross-sectional view of the simulated heterostructure is shown in Fig. 1(b), in which a 2DEG is formed 90 nm below the top surface (at the interface between the undoped AlGaAs layer and the lightly *p*-type doped GaAs layer).

We use computer modeling to simulate the correlation between the charging of the quantum states in the LCQD and the corresponding electrostatic variation in the QPC.[7] For this purpose, we solve coupled three-dimensional Kohn-Sham[8] and Poisson equations self-consistently to obtain the quantum states in the LCQD region, while outside this region the charge density is determined by solving Poisson equation within the Thomas-Fermi approximation.[7,9] The above differential equations are solved on a nonuniform three-dimensional (3D) mesh using the finite-element method (FEM) with proper boundary conditions, described elsewhere.[9,10] We use the Slater formula to determine the stable charge configuration in the LCQD,[11] which reads,

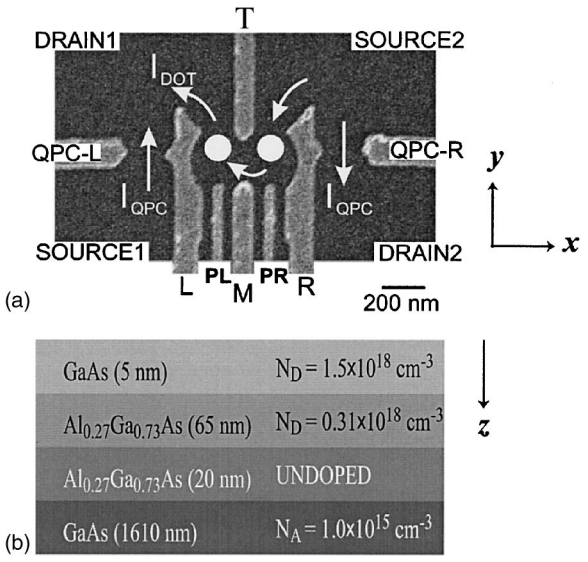

FIG. 1. (a) Scanning electron micrograph view of the top gates of the LCQD-QPC quantum circuit (light gray areas show the gate pattern for the LCQD and the QPC's, circles show the dots, curved arrows show the possible charging current paths, and straight arrows show the QPC currents). (b) Layers of the heterostructure (not to scale), after Elzerman *et al.* (Ref. 5).

a)Author to whom correspondence should be addressed; electronic mail: leburton@ceg.uiuc.edu

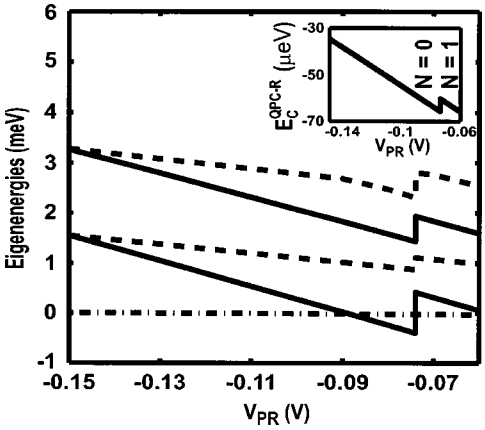

FIG. 2. Variation of the lowest four LCQD eigenenergies as a function of the right plunger gate bias V_{PR} (solid line: right dot; dashed line: left dot. The Fermi level is indicated as zero on the vertical scale). The inset shows the variation of the potential energy in the constriction of the right QPC as a function of V_{PR} (the vertical axis is shifted up by 0.0201 eV for clarity). $N=0(1)$ shows the electron number before (after) the charging (Ref. 7).

$$E_T(N+1)-E_T(N)=\int_0^1 \varepsilon_{LUO}(n)dn \approx \varepsilon_{LUO}\left(\tfrac{1}{2}\right)-E_F, \quad (1)$$

where $E_T(N)$ is the total energy for N electrons in the dots and $\varepsilon_{LUO}(1/2)$ is the eigenenergy of "the lowest unoccupied orbital," with half occupancy. The sign change of the right-hand side of Eq. (1), as a function of the tuning gate voltage, determines the electron occupation in the LCQD. In our simulation, we use a variation of the above rule where charging occurs when $\varepsilon_{LUO}(1)-E_F=E_F-\varepsilon_{LUO}(0)$, which was justified in Ref. 9.

Because of the circuit symmetry, we choose to charge the first electron into the right dot by varying only the right plunger gate bias.[7] In Fig. 2, starting from a gate bias configuration, where $V_L=V_R=V_{QPC-L}=V_{QPC-R}=V_M=-0.585$ V, $V_{PL}=V_{PR}=-0.15$ V, and $V_T=-0.9$ V (i.e., with zero electron in the LCQD), we change the right plunger gate bias until it reaches $V_{PR}=-0.06$ V (keeping other gate biases fixed), and record the changes of the lowest four eigenenergies in the LCQD accordingly. Simultaneously, we record the variation of the potential energy in the constriction of the right QPC(E_C^{QPC-R}) vs V_{PR} (see the inset of Fig. 2). As V_{PR} is made more positive, all the eigenenergies are lowered. At $V_{PR}=-0.074$ V, the ground-state energy in the LCQD is observed to have a discontinuity of 8.16×10^{-4} eV, bisected by the Fermi level (the Fermi level is set at zero throughout this work), which indicates the charging of the first electron in the right dot, as a result of the Slater formula in Eq. (1). An abrupt variation is also observed in the QPC potential energy at the same charging bias ($V_{PR}=-0.074$ V). This variation, ΔE_C, due to the Coulomb interaction between the right dot and the right QPC, results in the sudden changes in the conductance of the QPC(G) and the differential transconductance ($dI_{QPC}/dV_{plunger}$) vs $V_{plunger}$ observed experimentally.[4,5] From ΔE_C, we compute the relative change of the quantum conductance of the QPC detector at $G=G_0/2=e^2/h$ by

$$\frac{\Delta G}{G}=-\frac{\pi}{\hbar\omega_y}\Delta E_{C,} \quad (2)$$

where $\hbar\omega_y$ is the characteristic energy for a y-direction parabolic fitting of the potential energy near its saddle point in the constriction of the QPC.[7,12] In this study, the characteristic energy $\hbar\omega_y$ is obtained by fitting the potential energy in the constriction of the QPC with an 11-point parabola over the distance of the QPC gate (i.e., 1000 Å) along the y direction. Because of the high computational complexity of locating the halfway conductance point ($G_0/2$) precisely for the QPC detector, we instead compute the absolute value of the right-hand side of Eq. (2) within a wide experimental range of QPC gate biases (from −0.8 V to −0.3 V), aware that the condition $G=e^2/h$ falls within this range.

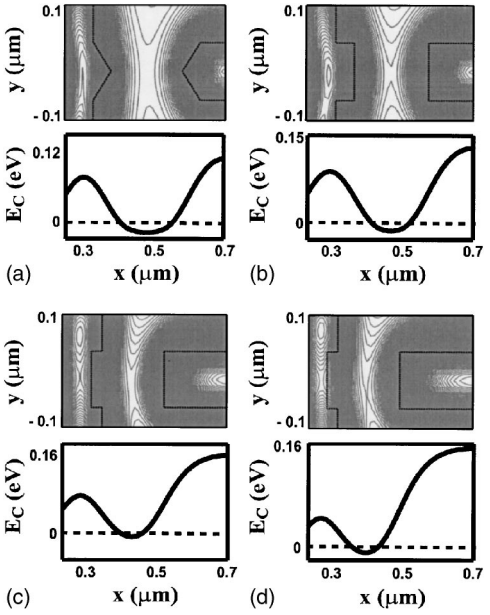

FIG. 3. (a), (b), (c), and (d): top panels: contour plots of the potential energy near the right QPC with the gate shape superimposed by dashed lines for design (a), (b), (c), and (d), respectively. Notice that equipotentials are lower (higher) in the channel (underneath the gates). Bottom panels: potential-energy profiles in the x direction at maximum QPC constriction ($y=-150$ Å). Dashed lines indicate the Fermi levels. The bias conditions are, in design (a), $V_L=V_R=V_M=-0.585$ V, $V_{PR}=-0.061$ V; in design (b), $V_L=V_R=V_M=-0.57$ V, $V_{PR}=-0.055$ V; in design (c), $V_L=V_R=V_M=-0.55$ V, $V_{PR}=-0.021$ V; in design (d), $V_L=V_R=V_M=-0.62$ V, $V_{PR}=-0.008$ V. Otherwise, $V_{PL}=-0.15$ V, $V_T=-0.9$ V, and $V_{QPC-L}=V_{QPC-R}=-0.8$ V for all the designs.

In Figs. 3(a)–3(d), we show four designs (a)–(d) of different QPC gate geometries (dark dashed lines in the upper panels) in a small region near the right QPC. In order to keep the symmetry of the circuit, we change the left QPC gates accordingly (not shown). Figure 3(a) shows the original design, while in Fig. 3(b), the tips of the QPC are replaced by flat ends to form a rectangular-shaped channel. In both Figs. 3(c) and 3(d), the detector is designed to have a dent in the R gate. In Fig. 3(d), the dent is placed 600 Å closer to the right QD than in Fig. 3(c). In these four designs, the nearest distance between the R gate and the QPC$-R$ gate is maintained at 2000 Å, which implies that for the design (d) the R gate is thinner in the dent while for design (c) it is thicker outside the dent. Equipotential-energy lines [gray solid lines in Figs. 3(a)–3(d) in the upper panels] are plotted under the gates showing the different conduction channel geometries caused by the different gate designs. The bias conditions for the circuit are specified in the figure captions for each case, and are chosen at the onset of the first electron charging in the right dot by changing V_{PR} over a fixed range (in our simulation, from −0.15 V to −0.1 V) for different QPC gate biases. It is clearly seen that the conduction channels in designs

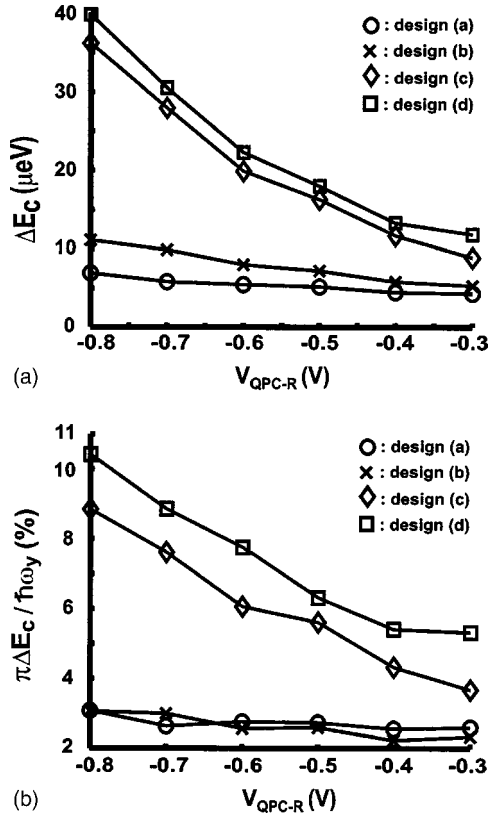

FIG. 4. (a) ΔE_C and (b) $|-(\pi/\hbar\omega_y)\Delta E_C|$ as a function of V_{QPC-R}. Different designs are labeled by different symbols shown on the figures. The characteristic energy $\hbar\omega_y$ is obtained by fitting the potential energy immediately before the charging of the first electron into the right QD, i.e., with zero electrons in the dot.

(b)–(d) are more squeezed compared to the channel in design (a). In Figs. 3(a) and 3(b) the channels are straight, while in Figs. 3(c) and 3(d) they are curved towards the right QD. The lower panels in Figs. 3(a)–3(d) show the potential-energy profiles along the x direction (for the same x distance as the upper panels). The conduction channels are seen to be increasingly confined from designs (a)–(c). Notice that the left potential-energy barrier for the QPC in design (d) is appreciably lower than the right one due to the small size of the R gate caused by the dent. However, this barrier remains wide enough, which should not cause any leaking of wave function between the right QD and QPC.

Starting from the bias configurations described in Fig. 3, we change the QPC-R gate bias V_{QPC-R} (the QPL$-L$ gate bias is also changed to maintain the symmetry of the quantum circuit) and record the ΔE_C change for different QPC gate biases, which is plotted in Fig. 4(a). We note that (1) for all the designs, ΔE_C decreases monotonically as V_{QPC-R} increases, which is due to the relaxation of the QPC confinement; (2) ΔE_C increases from design (a)–(d) at each QPC gate bias. This is because the conduction channels move closer to the right QD in each case. From the ΔE_C values in Fig. 4(a) and the ω_y fitting method, we obtain $|-(\pi/\hbar\omega_y)\Delta E_C|$ as a function of the QPC gate bias. In Fig. 4(b), it is shown that for designs (a) and (b), $|-(\pi/\hbar\omega_y)\Delta E_C|$ is rather insensitive to V_{QPC}, while it decreases monotonically as V_{QPC} is increased for designs (c) and (d). We notice that the detector sensitivity of the original design (a) ($\Delta G/G \approx 2\%$) is in good agreement with the experimental data.[5,7] The minimum values of $|-(\pi/\hbar\omega_y)\Delta E_C|$ for designs (c) and (d) (3.67% and 5.32%, respectively) are even larger than the maximum values of $|-(\pi/\hbar\omega_y)\Delta E_C|$ for designs (a) and (b) (3.07% and 3.06%, respectively) over the range of QPC gate biases. Hence, we conclude that for a specific QPC gate bias that achieves $G=G_0/2=e^2/h$, designs (c) and (d) have larger dectector sensitivity than designs (a) and (b). From the numerical values obtained in Fig. 4(b), we observe that the improvement of $|-(\pi/\hbar\omega_y)\Delta E_C|$ falls in the range from to $[\min(d)-\max(a)]/\max(a)=73\%$ to $[\max(d)-\min(a)]/\min(a)=308\%$, where $\min(a)$ and $\max(a)$ denote the minimum and maximum values achieved by $|-(\pi/\hbar\omega_y)\Delta E_C|$ for design (a) over the investigated voltage range and similarly for design (d).

This work is supported by the DARPA QUIST program through ARO Grant No. DAAD 19-01-1-0659. The authors thank P. Matagne for discussion, T. Saku and Y. Hirayama for fabricating the heterostructures, and the Material Computational Center at the University of Illinois through NSF Grant No. DMR-99-76550.

[1] B. J. van Wees, H. van Houten, C. W. J. Beenakker, J. G. Williamson, L. P. Kouwenhoven, D. van der Marel, and C. T. Foxon, Phys. Rev. Lett. **60**, 848 (1988).
[2] D. A. Wharam, T. J. Thornton, R. Newbury, M. Pepper, H. Ahmed, J. E. F. Frost, D. G. Hasko, D. C. Peacock, D. A. Ritchie, and G. A. C. Jones, J. Phys. C **21**, L209 (1988).
[3] M. Field, C. G. Smith, M. Pepper, D. A. Ritchie, J. E. F. Frost, G. A. C. Jones, and D. G. Hasko, Phys. Rev. Lett. **70**, 1311 (1993).
[4] D. Sprinzak, Y. Ji, M. Heiblum, D. Mahalu, and H. Shtrikman, Phys. Rev. Lett. **88**, 176805 (2002).
[5] J. M. Elzerman, R Hanson, J. S. Geidanus, L. H. Willems Van Beveren, S. De Franceschi, L. M. K. Vandersypen, S. Tarucha, and L. P. Kouwenhoven, Phys. Rev. B **67**, 161308(R) (2003).
[6] C. H. Bennett and D. P. DiVincenzo, Nature (London) **404**, 247 (2000).
[7] L.-X. Zhang, P. Matagne, J. P. Leburton, R. Hanson, and L. P. Kouwenhoven, Phys. Rev. B **69**, 245301 (2004). In this previous work, the characteristic energy $\hbar\omega_y$ was assumed to be constant and equal to 1 meV.
[8] W. Kohn and L. J. Sham, Phys. Rev. **140**, A1133 (1965).
[9] P. Matagne and J.-P. Leburton, Phys. Rev. B **65**, 235323 (2002).
[10] P. Matagne, J-P. Leburton, J. Destine, and G. Cantraine, Comp. Mod. Eng. Sciences **1**, 1 (2000).
[11] J. C. Slater, Adv. Quantum Chem. **6**, 1 (1972).
[12] M. Büttiker, Phys. Rev. B **41**, 7906 (1990).